

Processing Misregistered Hyperspectral Data

Jason T. Casey^b, Stephen R. Lach^{ab}, and John P. Kerekes^b

^aU.S. Air Force

^bChester F. Carlson Center for Imaging Science
Rochester Institute of Technology
54 Lomb Memorial Drive
Rochester, NY, USA 14623

ABSTRACT

Many hyperspectral sensors collect data using multiple spectrometers to span a broad spectral range. These spectrometers can be fed by optical fibers on the same or separate focal planes. The Modular Imaging Spectrometer Instrument (MISI), a 70 band line scanner built by the Rochester Institute of Technology, is configured in this manner. Visible and near infrared spectrometers at the primary focal plane are each fed by their own optical fiber. The spatial offset between the two fibers on the focal plane causes an inherent misregistration between the two sets of spectral bands. This configuration causes a relatively complicated misregistration which cannot be corrected with a simple shift or rotation of the data. This mismatch between spectral channels has detrimental effects on the spectral purity of each pixel, especially when dealing with the application of sub-pixel target detection. A geometric model of the sensor has been developed to solve for the misregistration and achieve image rectification. This paper addresses the issues in dealing with the misregistration and techniques used to improve spectral purity on a per pixel basis.

Keywords: registration, misregistration, target detection, spatial, spectral

1. INTRODUCTION

Hyperspectral imaging systems have become very useful in many fields because of their ability to capture the spectral nature of materials. Spectral features characteristic of objects manifest themselves in the way that materials absorb, transmit, scatter or reflect electromagnetic radiation. These materials may be identified by their spectral characteristics when using an airborne hyperspectral sensor.

Spectral imaging systems collect data in a variety of ways. Some imaging systems will capture an image a frame at a time, while selecting different filters in rapid succession to capture the spectral component of the scene over time. A pushbroom sensor captures data one line at a time, separating incoming electromagnetic radiation into narrow continuous wavelengths, or bands across a 2 dimensional array. In these systems each band is captured simultaneously in a single line. Many lines are captured over time, creating an image as the aircraft moves forward. Probably the simplest imaging system is the line scanner. A line scanner employs a rotating scan mirror which scans out a line of data on the ground. The data in a line is collected one pixel at a time, while the spectral component of each pixel is collected simultaneously though dispersion across a linear array.

Each type of imaging system has benefits over another, as well as trade-offs. Systems which collect a spectrum over time have to deal with the issue of scene dynamics affecting the spectral character of each pixel while the aircraft and objects in the scene are moving. Linear array sensors, as well as line scanners do not capture the spatial makeup of the scene all at once. Problems here arise when attempting to register data to a gridded coordinate system. Aircraft attitude changes during the image capturing process, and results in the formation of non-rectilinear images. Line scanners often utilize multiple focal planes, or employ multiple optical fibers on the same focal plane. These optical fibers usually feed separate spectrometers. Such systems suffer from an inherent

Further author information: (Send correspondence to J.T.C.)

J.T.C.: E-mail: jtc6922@cis.rit.edu, Telephone: 1 607 206 6644

J.P.K.: E-mail: Kerekes@cis.rit.edu, Telephone: 1 585 475 6996

spatial misregistration issue. Since the optical fibers are not in the same location on the focal plane, they image slightly different points on the ground.

The work set forth in this paper attempts to correct for the misregistration issue between bands of one sensor that has been designed and built at the Rochester Institute of Technology. The Modular Imaging Spectrometer Instrument (MISI) employs two optical fibers each at the primary focal plane, one feeding a visible spectrometer, and one feeding a near infrared spectrometer. These fibers are placed roughly 6mm apart, which causes a spatial misregistration between the sets of bands.

2. MISI DESCRIPTION AND DESIGN

Over almost 15 years, MISI has been designed, built and maintained by contributions from staff and students at the Center for Imaging Science. MISI supports a variety of remote sensing applications, including target detection experiments, studying cloud effects on atmospheric compensation techniques, and supporting LANDSAT calibration studies over Lake Ontario.

MISI is a hyperspectral line scanner equipped with a fold mirror, a 6 inch rotating scan mirror and a Cassegrain telescope which has a focal length of 0.5m. Incident electromagnetic radiation is reflected off MISI's rotating scan mirror as it sweeps out a field of view of $\pm 45^\circ$. This gives the instrument a 4 km FOV when flying at an altitude of 2000m AGL. The light passes through a cassegrainian telescope, and is then separated onto three separate focal planes. The primary focal plane, as mentioned before, contains optical fibers leading to visible (VIS) and near-infrared (NIR) spectrometers. The other two focal planes are for used for midwave infrared (MWIR) and long wave infrared (LWIR) channels. The primary focus of this paper will cover the optical fibers at the primary focal plane. Table 1 provides instrument specifications. Image (a) in Figure 1 shows MISI on top of one of the academic buildings and image (b) shows the optical components of MISI in some more detail.

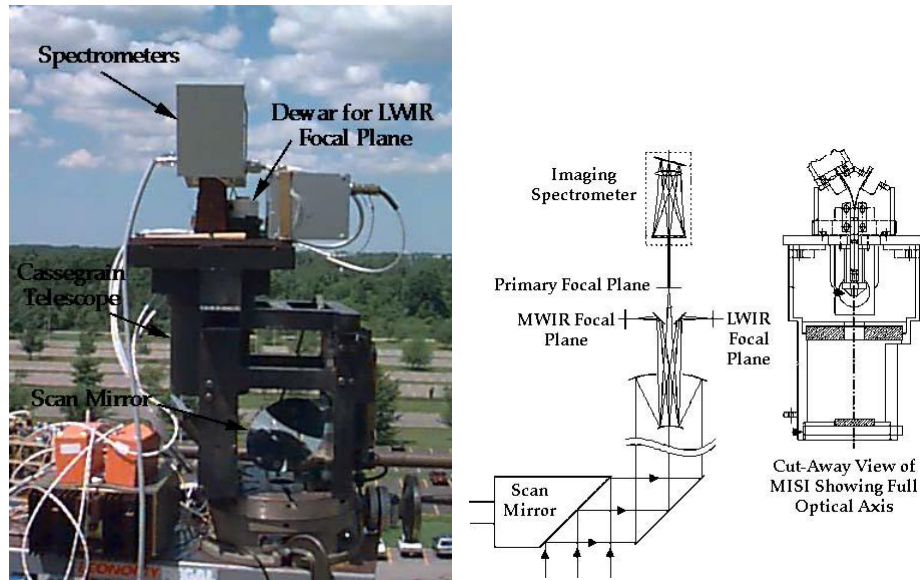
Table 1. MISI specifications

Spectral Band	Center λ	# Channels	$\Delta\lambda$	GIFOV @ 2000' AGL
VIS	0.41 - 0.75 μm	35	0.012 μm	6'
NIR	0.74 - 1.02 μm	35	0.010 μm	6'
SWIR	1.26 μm	1	0.11 μm	4'
SWIR	1.65 μm	1	0.38 μm	4'
SWIR	2.03 μm	1	0.65 μm	4'
MWIR	3.65 μm	1	0.9 μm	4'
LWIR	9 μm	1	2 μm	4'
LWIR	11 μm	1	2 μm	4'
LWIR	11.5 μm	1	2.1 μm	4'
LWIR	11 μm	1	6 μm	2'

As stated above, there is an inherent misregistration between the VIS and NIR bands due to MISI's design. The VIS and NIR spectrometers are each fed by their own optical fiber. Both lie on the primary focal plane, but they are in different locations, separated by roughly 6mm. This separation is responsible for the misregistration between bands.

3. DATA COLLECTION

MISI is routinely flown over RIT's campus to support various remote sensing experiments. One of these experiments took place on October 6th, 2005 as a continuation of a vehicle tracking effort.¹Volunteers positioned vehicles relatively close together near a set of painted calibration panels in a parking lot. MISI was flown over the campus to collect data, and the vehicles changed locations and recorded their positions between repeat passes. Spectral ground measurements of the vehicles and the calibration panels were made. Previous experiments similar to this showed promising results for vehicle tracking by applying a spectral matched filter to data using vehicle spectra collected from a pixel in the previous image.



(a) MISI on top of one of the academic buildings at RIT

(b) A side view of MISI

Figure 1. Two views of the Modular Imaging Spectrometer Instrument.

Another experiment was performed on October 10th, 2006, to help determine the amount of spatial misregistration between bands was present in the raw MISI imagery. Identifying features, as well as highly reflective targets placed on the ground were chosen to determine the severity of the spatial shift.

3.1. Spatial Shift Between Spectral Bands

When analyzing all the MISI datasets, it was noted that the shift between the VIS and NIR bands was not a simple uniform shift, but rather a more complex shift that appeared to change across the image. This behavior suggested that the amount of vertical and horizontal shift in the image could be expressed as a function of the scan angle of MISI's scan mirror. The effects of the shift could be seen very clearly when linking displays to one another, but is much harder to observe when the images are placed side by side. Several zoomed in images with ground points have been provided to give the reader a better understanding of the spatial misregistration.

Figure 2 is a color image created from 3 of MISI's visible bands. This happens to be a raw image from the sensor, and appears wider than a normal image due to the fact that MISI oversamples in the across track direction. The waviness in the image is due to the fact that no roll correction has been applied.

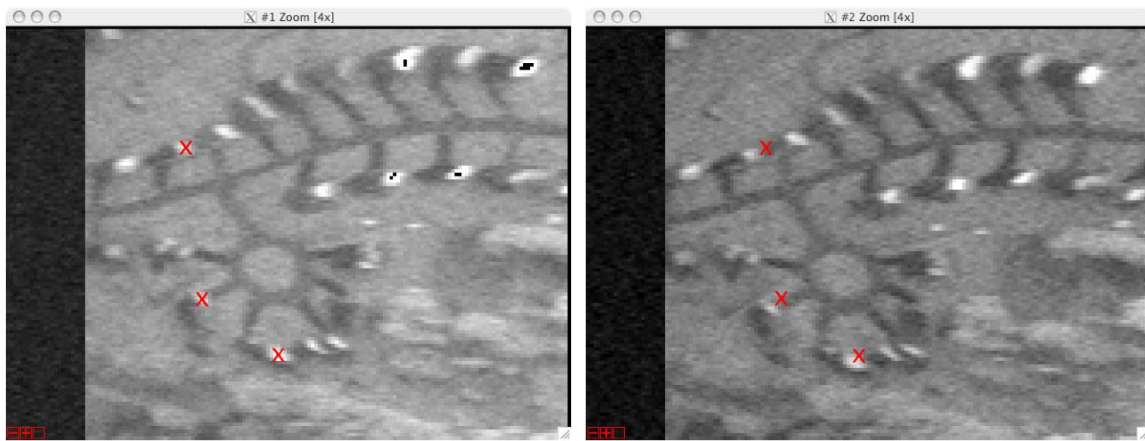
Figures 3 and 4 show the misregistration in the raw MISI data. The X's mark the same pixel index in the two images. As can be seen from the figures, there is a misregistration of several pixels between features in each band. At the left hand side of the image (Figure 3), the near infrared bands appear to shift lower vertically and to the left relative to the visible bands. The type of shift changes as the image is scanned from left to right. Toward the center of the image, the horizontal shift increases, while the vertical shift becomes much less prevalent. At the right hand side of the image (Figure 4), the vertical shift changes, so the near infrared features appear to shift higher vertically relative to the visible features. To better understand what causes this, a geometric model of MISI was created.

4. MISI GEOMETRIC MODEL

A geometric model of MISI was created in order to demonstrate and understand the effects the optical system has on the misregistration between bands. A general case was developed to trace a ray from a location on the



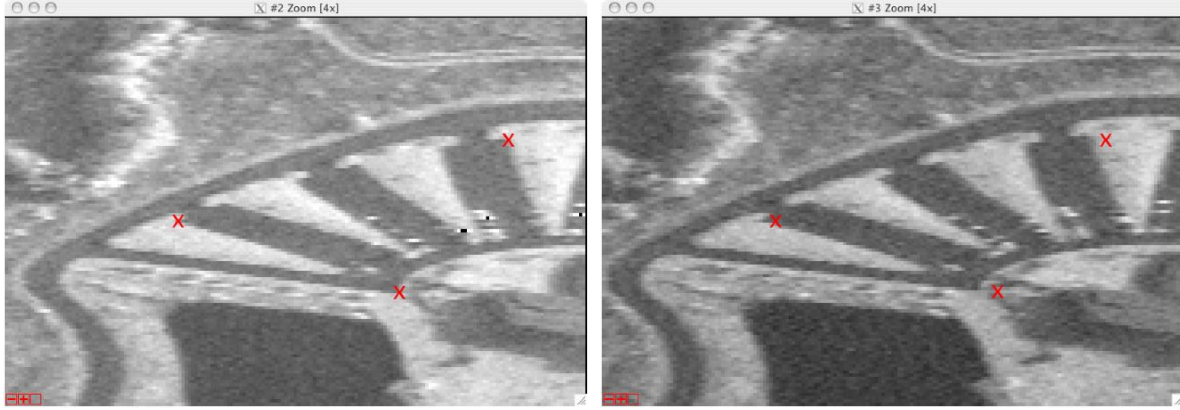
Figure 2. Raw, un-roll-corrected color rendition of the scene of interest taken by MISI.



(a) Visible band, left side of image

(b) Near infrared band, left side of image

Figure 3. Spatial misregistration between VIS and NIR bands at the right side of the image. The X's in the images denote the same pixel location.



(a) Visible band, right side of image

(b) Near infrared band, right side of image

Figure 4. Spatial misregistration between VIS and NIR bands at the right side of the image. The X's in the images denote the same pixel location.

primary focal plane through the optical system of the sensor to determine the direction the ray would point from the rotating scan mirror.

4.1. Developing a coordinate system

For convenience, a single coordinate system was chosen when tracing rays through the optical system. A 3 dimensional coordinate system was chosen with the x axis as the along track direction, or the direction of aircraft flight during data collection. The y axis was chosen to point toward the left wing of the aircraft as seen from the pilots perspective, and the z axis was chosen to point upward. The origin was placed at the center of the primary focal plane, with the z axis passing through the "optical center" of the cassegranian telescope.

4.2. Tracing a ray through the telescope

The first step in constructing the geometric model was determining how light passes through the optical system and onto the focal plane. The focal length of $0.5m$ was known, but the exact configuration of the telescope was not. When using lenses to focus light, rays can be traced through the optical center of the lens. When using mirrors, rays may be traced through the center of curvature of the mirror.² The "optical center" of the cassegranian telescope was unknown, and several experiments were required for it to be approximated. All rays were represented with unit vectors, and the first ray passing through the optical center, is written as

$$\hat{A} = \frac{[-x_0, -y_0, -f]}{\sqrt{x_0^2 + y_0^2 + f^2}} \quad (1)$$

where x_0, y_0 is the location of the fiber on the focal plane, and f is the distance from the focal plane to the optical center. The reader may refer to Figure 5 to find each ray defined in this section.

4.3. Rotation about first fold mirror

After the ray is traced through the optical center, it intersects with a fold mirror. The ray will reflect off this surface. The normal to the fold mirror is given as

$$\hat{N}_1 = \left[-\frac{\sqrt{2}}{2}, 0, \frac{\sqrt{2}}{2} \right] \quad (2)$$

The equation for a ray reflecting off a surface may be determined by negating it and rotating about the normal vector. The resulting reflected vector is written as

$$\hat{B} = 2 \left[-\hat{A} \cdot \hat{N}_1 \right] \hat{N}_1 + \hat{A} \quad (3)$$

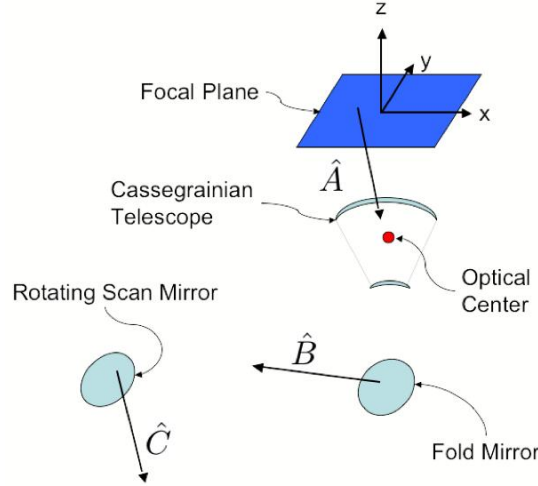


Figure 5. Rays traced through MISI's optical system.

4.4. Rotation about rotating scan mirror

The scan mirror, unlike the stationary fold mirror, rotates to collect lines of data. In a fixed coordinate system, this means the normal vector to the scan mirror changes as a function of the scan angle. This normal vector to the scan mirror may be described as

$$\hat{N}_2 = \left[\frac{\sqrt{2}}{2}, \frac{\sqrt{2}}{2} \cos \theta, -\frac{\sqrt{2}}{2} \sin \theta \right] \quad (4)$$

where θ is the angle of rotation of the scan mirror. Keeping in mind that \hat{N}_2 is a function of θ , \hat{B} may be reflected off this mirror in the same way \hat{A} is reflected off the fold mirror. The resulting reflected vector can be written as

$$\hat{C} = 2 \left[-\hat{B} \cdot \hat{N}_2 \right] \hat{N}_2 + \hat{B} \quad (5)$$

This was the last step in constructing the geometric model. From here, \hat{C} can be projected to the ground location where data is collected.

5. CORRECTION EXPERIMENTS

One method for co-registration is to use the geometric model to determine the amount of shift between pixels as a function of the scan angle. If it is assumed that the sensor orientation does not change much between scan lines, this shift can be applied on a pixel by pixel basis in the image. The amount of misregistration was calculated using the resulting vectors off the scan mirror for each pixel in a scan line. Little documentation was available for MISI, but the optical fibers were believed to be separated by roughly $6mm$ in the along track position (both lying on the Y axis). The optical center was unknown, but after several registration attempts, the optical center appeared to lie close to $0.05m$ from the focal plane. For each sampled across-track pixel, the resulting vectors \hat{C}_{VIS} and \hat{C}_{NIR} were calculated. These vectors were broken up into their $X-Z$ and $Y-Z$ planar components. Keep in mind in the current coordinate system, Y denotes the across track direction, while X denotes the along track direction, which may be counter-intuitive when looking at an image. The angles of separation were computed as:

$$\gamma_x = \arccos \left(\frac{VIS_{X-Z} \cdot NIR_{X-Z}}{|VIS_{X-Z}| |NIR_{X-Z}|} \right) \quad (6)$$

$$\gamma_y = \arccos \left(\frac{VIS_{Y-Z} \cdot NIR_{Y-Z}}{|VIS_{Y-Z}| |NIR_{Y-Z}|} \right) \quad (7)$$

where VIS_{X-Z} , NIR_{X-Z} are the components of the \hat{C}_{VIS} and \hat{C}_{NIR} vectors in the $X-Z$ plane, and VIS_{Y-Z} , NIR_{Y-Z} are the components of the \hat{C}_{VIS} and \hat{C}_{NIR} vectors in the $Y-Z$ plane. Knowing the across-track field

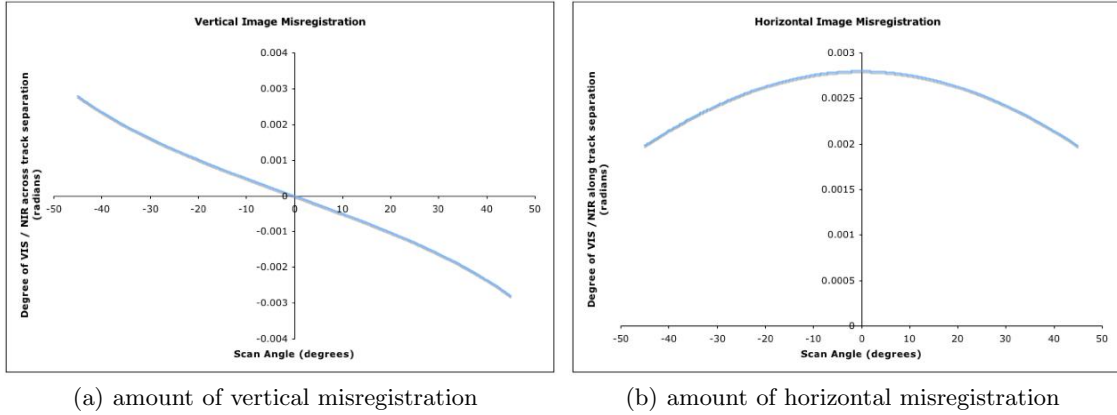


Figure 6. Amount of horizontal and vertical misregistration in a scan line for a plane flying straight and level. The X axis represents the angle of the scan mirror from -45 to +45 degrees. The Y axis represents the amount of spatial misregistration in radians.

of view was 90° , the number of pixels to be shifted was calculated by

$$pixels_y = \frac{\gamma_y \times n_{across-track}}{\frac{\pi}{2}} \quad (8)$$

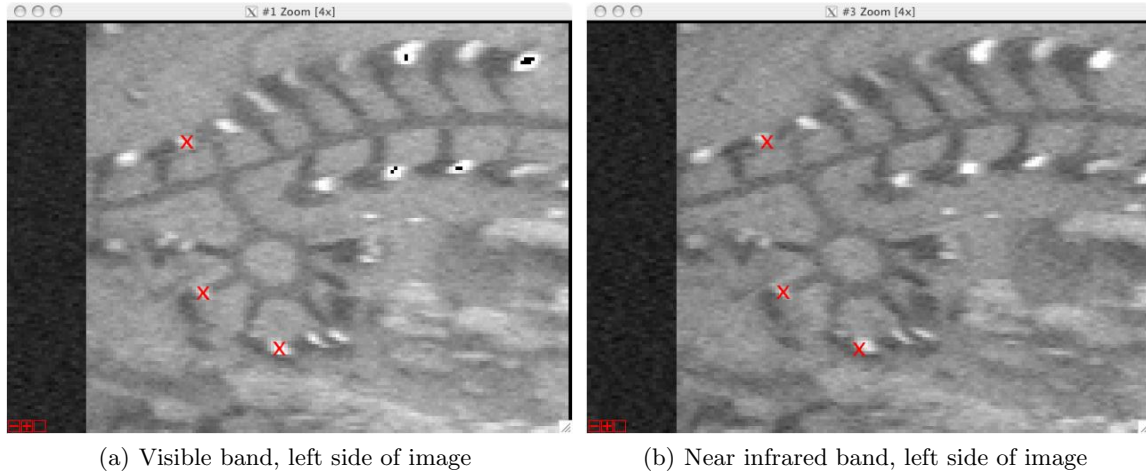
Where $n_{across-track}$ is 2150 pixels. MISI is configured to oversample in the across track direction. From observations in the image, and from some initial results, it appeared that approximately 1.5X oversampling was occurring in the across track direction. This approximation was used to determine the number of pixels that should be shifted in the along track direction. Figure 6 demonstrates how the vertical and horizontal shift varies as a function of the scan angle.

$$pixels_x = \frac{\gamma_x \times \frac{1}{1.5} n_{across-track}}{\frac{\pi}{2}} \quad (9)$$

The VIS bands were used as a reference, and the appropriate shifts were applied to the NIR bands of the image. The X's in Figures 7 and 8 represent the same pixels in each respective image. Features in both sets of bands appear to align much better than before any correction was made. Notice, however that as some points match up very closely between bands, but some features are still shifted up to several pixels. There seems to be no particular shifting pattern after co-registration has been applied to the NIR bands. This is because one of the assumptions made was that sensor orientation does not change much between small numbers of lines, which is not always a good assumption.

6. IMPROVING CO-REGISTRATION

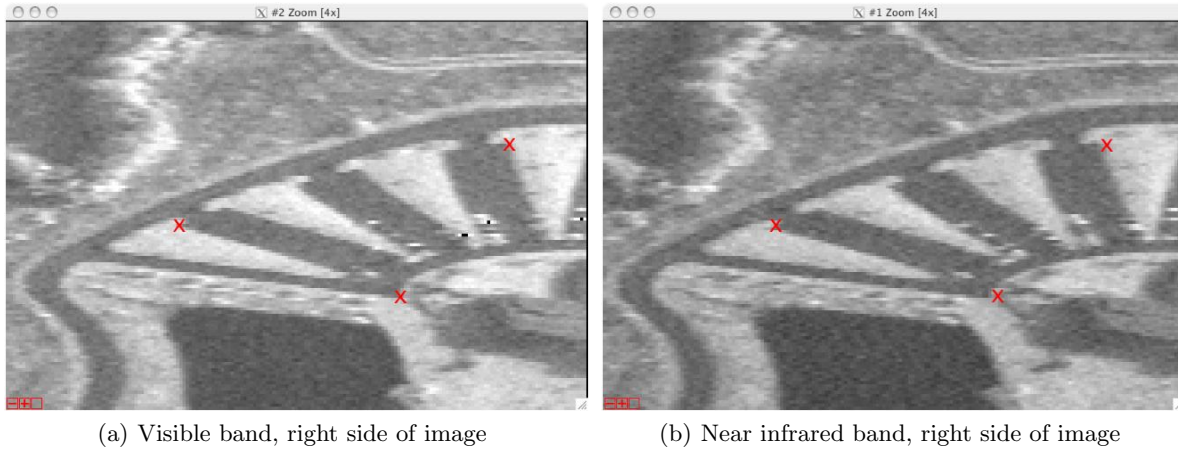
A method by Wanpeng Zhang has been proposed for creating georegistered images from line scanner data.³ Onboard flight parameters are used to project each collected pixel onto the earth. Using this method UTM coordinates may be computed for every pixel in an image, and the line scanner imagery may be manipulated to create a georectified image. For this method to be feasible, accurate GPS measurements of the aircraft, as well as orientation angles must be known. Applying this idea and using the MISI geometric model, UTM coordinates may be computed for every pixel in each band. Using an image from a visible band, it is possible to find corresponding pixels in a NIR band which has been assigned the closest UTM coordinate to their respective VIS pixels. Using this method, the sensor geometric model, as well as aircraft orientation (roll, pitch and yaw) can be accounted for. If a digital elevation model (DEM) of the scene is available, effects due to terrain can be



(a) Visible band, left side of image

(b) Near infrared band, left side of image

Figure 7. Spatial misregistration between VIS and NIR bands at the right side of the image after co-registration has been applied to the images. The X's represent the same pixel index between the VIS and NIR bands.



(a) Visible band, right side of image

(b) Near infrared band, right side of image

Figure 8. Spatial misregistration between VIS and NIR bands at the right side of the image after co-registration has been applied.

accounted for as well. This is done by intersecting each vector off the sensor with the DEM to determine the ground coordinates of each collected pixel.

Aircraft roll (ω), pitch (ϕ) and yaw (κ) were considered in the improved model. A transformed coordinate system accounting for roll, pitch and yaw may be found by multiplying a ground-looking vector by each operator in order. Still using the defined coordinate system, the roll operator may be written as:

$$roll = \begin{bmatrix} 1 & 0 & 0 \\ 0 & \cos(\omega) & \sin(\omega) \\ 0 & -\sin(\omega) & \cos(\omega) \end{bmatrix} \quad (10)$$

the pitch operator may be written as:

$$pitch = \begin{bmatrix} \cos(\phi) & 0 & -\sin(\phi) \\ 0 & 1 & 0 \\ \sin(\phi) & 0 & \cos(\phi) \end{bmatrix} \quad (11)$$

the yaw operator may be written as:

$$yaw = \begin{bmatrix} \cos(\kappa) & \sin(\kappa) & 0 \\ -\sin(\kappa) & \cos(\kappa) & 0 \\ 0 & 0 & 1 \end{bmatrix} \quad (12)$$

by multiplying these operators together, a rotation matrix, M is derived.

$$M = \begin{bmatrix} m_{11} & m_{12} & m_{13} \\ m_{21} & m_{22} & m_{23} \\ m_{31} & m_{32} & m_{33} \end{bmatrix} \quad (13)$$

where m 's listed below have been substituted for the resulting coefficients from the matrix multiplication.

$$\begin{aligned} m_{11} &= \cos(\phi) \cos(\kappa) \\ m_{12} &= \sin(\omega) \sin(\phi) \cos(\kappa) + \cos(\omega) \sin(\kappa) \\ m_{13} &= -\cos(\omega) \sin(\phi) \cos(\kappa) + \sin(\omega) \sin(\kappa) \\ m_{21} &= -\cos(\phi) \sin(\kappa) \\ m_{22} &= -\sin(\omega) \sin(\phi) \sin(\kappa) + \cos(\omega) \cos(\kappa) \\ m_{23} &= \cos(\omega) \sin(\phi) \sin(\kappa) + \sin(\omega) \cos(\kappa) \\ m_{31} &= \sin(\phi) \\ m_{32} &= -\sin(\omega) \cos(\phi) \\ m_{33} &= \cos(\omega) \cos(\phi) \end{aligned}$$

A forward transformation produces vectors in the transformed space, that is, in the sensor's frame of reference. The opposite is actually desired, that is, to know where the sensor is pointing with respect to the world coordinate system so each pixel can be projected to the ground. The rotation matrix is an orthonormal matrix, which has the property that its inverse is equal to its transpose.⁴ This means

$$M^{-1} = M^T \quad (14)$$

M^T may now be used to operate on \hat{C} to compute the ground-pointing vectors for each pixel.

$$\hat{C}' = C'_x, C'_y, C'_z = M^T \hat{C} \quad (15)$$

If a DEM is not available, a flat earth may be assumed. Vectors may be projected onto a local ground coordinate system by

$$X_{loc} = T_x - \frac{\hat{C}'_x}{C'_z} H \quad (16)$$

$$Y_{loc} = T_y - \frac{\hat{C}'_y}{C'_z} H \quad (17)$$

where T_x and T_y are the X and Y coordinates of the aircraft relative to a ground-based coordinate system with X pointing in the direction of aircraft flight.

7. ONGOING WORK

The aircraft orientation model shown above was implemented to produce georectified, roll-corrected images. More work is needed to complete band to band registration using this technique. Assuming coregistration within 1 pixel is achievable, more robust target detection algorithms are being pursued which take into consideration the background mixing uncertainty in one set of bands. This is important because perfect coregistration is never achievable. Since the pixels corresponding to the same ground location for the VIS and NIR bands are collected at different times, no two pixels will ever represent the exact same spot on the ground.

8. ACKNOWLEDGMENT

Acknowledgment is made to Tim Gallagher and Rolando Raqueño for providing information about MISI, and Don McKeown, who contributed significantly to the creation of the MISI geometric model.

This material is based on research sponsored by AFRL/SNAT under agreement number FA8650-04-1-1717 (BAA 04- 03-SNK Amendment 3). The U.S. Government is authorized to reproduce and distribute reprints for Governmental purposes notwithstanding any copyright notation thereon. The views expressed in this article are those of the authors and do not reflect the official policy or position of the United States Air Force, the Department of Defense, or the U.S. Government.

REFERENCES

1. J. Kerekes, M. Muldowney, K. Strackerjan, L. Smith, and B. Leahy, "Vehicle tracking with multi-temporal hyperspectral imagery," *Proceedings of Algorithms and Technologies for Multispectral, Hyperspectral and Ultraspectral Imagery XII* **6233**, p. 9, 2006.
2. E. Hecht, *Optics*, Addison Wesley, 4 ed., August 2001.
3. W. Zhang and J. Albertz, "Rectification of airborne line-scanner imagery utilizing flight parameters," First International Airborne Remote Sensing Conference and Exhibition, (Strasbourg, France), 1994.
4. P. R. Wolf and B. A. Dewitt, *Elements of Photogrammetry with Applications in GIS*, McGraw hill, 3 ed., February 2000.